

Inviscid Solutions of the Flowfield in an Internal Combustion Engine

R. Diwakar,* John D. Anderson Jr.,† Michael D. Griffin,* and Everett Jones‡

University of Maryland, College Park, Md.

Theme

THIS paper is a direct companion to that of Griffin et al.¹ In Ref. 1, the complete Navier-Stokes equations were applied to the solution of the viscous flowfield inside an internal combustion engine for a complete 4-stroke cycle—intake, compression, power, and exhaust. The major problem with such solutions is their restriction to low Reynolds numbers in order to remain within practical computer times. In contrast, the present paper investigates the *inviscid* flowfield in an IC engine. Some advantages of an inviscid solution are: 1) full-scale engines running under atmospheric conditions can be readily treated in reasonably practical computer times; 2) the true flowfield inside real IC engines might be reasonably modeled via a large inviscid core plus a viscous boundary layer at the walls, as conventionally done in aerodynamics; and 3) an inviscid solution might be the most practical vehicle for initial studies of the interaction between the flowfield and the combustion processes.

Contents

The piston-cylinder-valve geometry is illustrated in Fig. 1 of Ref. 1. The pressure, temperature, density, and velocity distributions between the top of the cylinder and the face of the piston are calculated as functions of space and time throughout the complete intake, compression, power, and exhaust strokes. As in Ref. 1, the flow is two-dimensional (an infinite aspect ratio engine). Such 2-D calculations are appropriate for a first-generation analysis, and they bring out the basic aspects of the fluid dynamics inside the cylinder. Combustion is not treated in detail; rather, the temperature at the top of the compression stroke is increased artificially to simulate combustion. The compressible Euler equations are solved at each grid point (a 10×9 grid is used) by means of a time-dependent finite-difference technique patterned after MacCormack.² Unlike Ref. 1, slip boundary conditions are employed at the surface. Also, p and T are variable at the intake valve. The present inviscid solutions are much more sensitive to the valve boundary conditions than the viscous solutions of Ref. 1. Indeed, the valve boundary conditions represent the most critical factor affecting the present inviscid solutions; they are discussed in detail in the full paper.

Figures 1-4 give the inviscid velocity patterns for the intake, compression, power, and exhaust strokes, respectively. In contrast to the highly viscous results of Ref. 1, these patterns

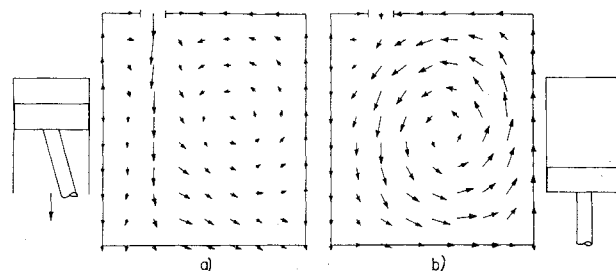


Fig. 1 Velocity pattern—intake stroke: 600 rpm; a) 90° from top dead center (TDC); b) bottom dead center (BDC).

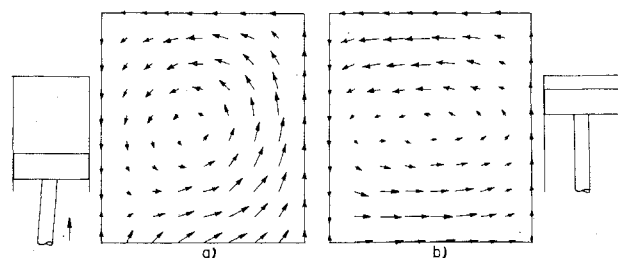


Fig. 2 Velocity pattern—compression stroke: 600 rpm; a) 30° from BDC; b) TDC.

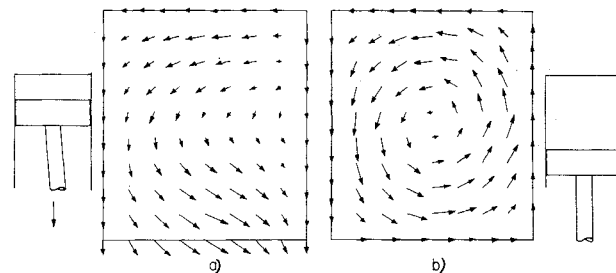


Fig. 3 Velocity pattern—power stroke: 600 rpm; a) 30° from TDC; b) BDC.

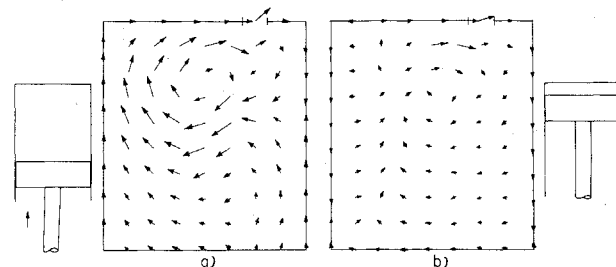


Fig. 4 Velocity pattern—exhaust stroke: 600 rpm; a) 20° from BDC; b) TDC.

Received June 10, 1976; synoptic received Aug. 27, 1976. Full paper available from National Technical Information Service, Springfield, Va., 22151 as N-76-31457 at the standard price (available upon request). This work was supported by the Minta Martin Fund for Aeronautical Research, an endowment given to the College of Engineering, University of Maryland, by the late Glenn L. Martin. Computer time was provided through the facilities of the Computer Science Center of the University of Maryland.

Index category: Airbreathing Propulsion, Subsonic and Supersonic.

*Graduate Research Assistant, Department of Aerospace Engineering, Student Member AIAA.

†Professor and Chairman, Department of Aerospace Engineering, Associate Fellow AIAA.

‡Associate Professor, Department of Aerospace Engineering, Member AIAA.

show strongly circulating flows throughout the complete 4-stroke cycle. These figures are self-explanatory, and should be compared with Figs. 2-5 of Ref. 1. These circulating flows must have some effect on the combustion processes in a real

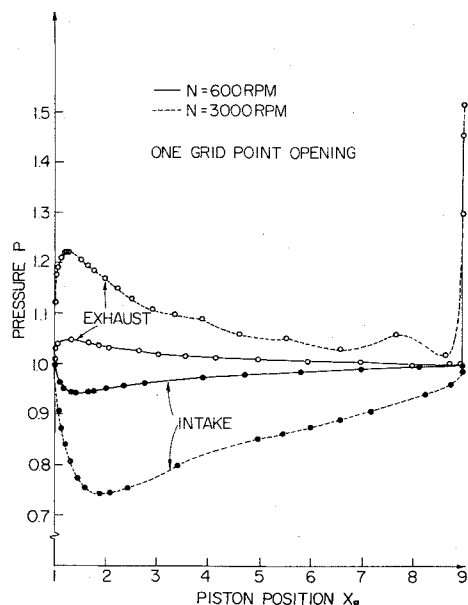


Fig. 5 Comparison of p - x diagrams for exhaust and intake for small and large RPM; $x=2$, $y=2$.

engine. Pressure, temperature, and density variations also are obtained. An example is given in Fig. 5, which illustrates the pressure at $x=2$ and $y=2$ as a function of piston location for the intake and exhaust strokes, comparing high and low rpm.

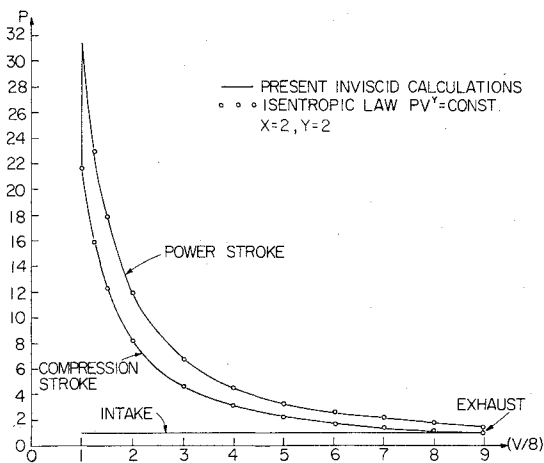


Fig. 6 Indicator diagram: 600 rpm.

Also, Fig. 6 shows an indicator diagram comparing the present 2-D calculation with the ideal Otto cycle.

References

- ¹Griffin, M.D., Anderson, J.D., Jr., and Diwaker, R., "Navier-Stokes Solutions of the Flowfield in an Internal Combustion Engine," AIAA Paper 76-403. Also, *AIAA Journal*, Vol. 14, Dec. 1976, pp. 1665-1666.
- ²MacCormack, R.W., "The Effect of Viscosity in Hypervelocity Impact Cratering," AIAA Paper 69-354, Cincinnati, Ohio, 1969.

Announcement: 1976 Author and Subject Index

The indexes of the four AIAA archive journals (*AIAA Journal*, *Journal of Spacecraft and Rockets*, *Journal of Aircraft*, and *Journal of Hydronautics*) will be combined and mailed separately early in 1977. In addition, papers appearing in volumes of the *Progress in Astronautics and Aeronautics* book series published in 1976 will be included. Librarians will receive one copy of the index for each subscription which they have. Any AIAA member who subscribes to one or more Journals will receive one index. Additional copies may be purchased by anyone, at \$10 per copy, from the Circulation Department, AIAA, Room 730, 1290 Avenue of the Americas, New York, New York 10019. **Remittance must accompany the order.**

Ruth F. Bryans
Director, Scientific Publications